자원환경지질, 제34권, 제6호, 507-522, 2001
Econ. Environ. Geol., 34(6), 507-522, 2001

# Au-Ag-Te Mineralization by Boiling and Dilution of Meteoric Groundwater in the Tongyeong Epithermal Gold System, Korea: Implications from Reaction Path Modeling

**Maeng-Eon Park[1]*, Kyu-Youl Sung[1] and Laurence P. James[2]**

*[1]Department of Environmental Geosciences, Pukyoung National University,Busan, 608-737, Republic of Korea*
*[2]James Geoassociates, Lakewood, Colorado, USA And University of Colorado, Boulder Campus, 80309-0399, USA*

# 광화유체의 비등과 희석에 의한 통영 천열수계 Au-Ag-Te 광화작용에 대한 반응경로 모델링

**박맹언[1]* · 성규열[1] · Laurence P. James[2]**

[1]부경대학교 환경지질과학과, [2]콜로라도대학

통영광산은 천열수광상으로서 능망간석, 백운모, 일라이트, 황철석, 방연석, 황동석, 섬아연석, 아칸다이트 및 헤사이트 등의 광물을 수반하는 초기의 광석광물 침전시기와 후기의 맥석광물 침전시기로 구분된다. 초기는 반복적인 대상구조를 띠고, 황화광물이 침전된 시기로서 텔루리움 광물과 함께 엘렉트럼이 산출된다. 후기에는 주로 탄산염 광물과 천금속광물이 침전되었다. 통영 열수계에서 광화단계에 따른 상이한 열수유체의 변천과정을 구체적으로 규명하기 위하여 프로그램 CHILLER를 이용한 수치모델링이 실시되었다. 반응경로 모델링은 280°C에서 모암인 안산암과의 반응을 비롯하여, 260°C에서 120°C까지의 단순한 등압 냉각, 비등과 지하수의 혼입에 따른 희석 및 압력과 온도가 감소되는 조건에서 수행하였다. 모델링 결과 초기 광화유체는 산성용액(pH=5.7)으로 상대적으로 높은 염농도와 금속원소 함량이 높다. 광화유체 내의 금의 함량은 열수계의 천금속원소 총량과 황화물의 활동도에 의해 지배된다. 통영 천열수계에서의 광화작용은 천부에서 일어난 광화유체의 비등과 이에 수반된 가열된 지하수의 혼입에 의한 반응경로를 반영하며, 현미경에서 관찰된 광물공생 특성과 모델링에 의한 침전광물의 조합 및 엘렉트럼의 화학조성 등에서 동일한 경향을 나타낸다. 이러한 유사성은 Te 함유하는 천열수 금 · 은광상이 열수계에서의 비등과 유체혼합(희석)에 의해 생성되었음을 지시한다. 반응경로 모델링 연구는 광상성인을 이해하는 중요한 수단이며, 유사한 지질환경에서의 광상탐사에 유용한 자료로 활용될 것으로 생각된다.

**주요어** : 반응경로모델링, 천열수금, Te 함유 금광상, 통영광산, 비등과 희석, 지구화학 탐사

At the Tongyeong mine, quartz, rhodochrosite (kutnahorite), muscovite, illite, pyrite, galena, chalcopyrite, sphalerite, acanthite, and hessite are the principal vein minerals. They were deposited under epithermal conditions in two stages. Ore mineral assemblages and associated gangue phases in stage can be clearly divided into two general associations: an early cycle (band) that appeared with introduction of most of the sulfides and electrum, and a later cycle in which base metal and carbonate-bearing assemblages (mostly rhodochrosite) became dominant. Tellurides and some electrum occur as small rounded grains within subhedral-to euhedral pyrite or anhedral galena in stageII. Sulfide mineralization is zoned from pyrite to galena and sphalerite. We have used computer modeling to simulate formation of four stages of vein genesis. The reaction of a single fluid with andesite host rock at 280°C, isobaric cooling of a single fluid from 260°C to 120°C, and boiling and mixing of a fluid with both decreasing pressure and temperature were studied using the CHILLER program. Calculations show that the precipitation of alteration minerals is due to fluid-andesite interaction as temperature drops. Speciation calculations confirm that the hydrothermal fluids with moderately high salinities and pH 5.7 (acid), were capable of transporting significant quantities of base metals. The abundance of gold in fluid depends critically on the ratio of total base metals and iron to sulfide in the aqueous phase because gold is transported as an $Au(HS)_2^-$ complex, which is sensitive to sulfide activity. Modeling results for Tongyeong mineralization show strong influence of shallow hydrogenic processes such as boiling and fluid mixing. The variable banding in stageII mineralization is best explained by mul-

*Corresponding author: mepark@pknu.ac.kr

tiple boilings of hydrothermal fluid followed by lateral mixing of the fluid with overlying diluted, steam-heated ground water. The degree of similarity of calculated mineral assemblages and observed electrum composition and field relationships shows the utility of the numerical simulation method in identifying chemical processes that accompany boiling and mixing in Te-bearing Au-Ag system. This has been applied in models to narrow the search area for epithermal ores.

Key words : reation path modeling, epithermal gold, Te-bearing Au-Ag, Tongyeong mine, boiling and mixing, geochemical exploration

## 1. INTRODUCTION

Most of the Korean Peninsula and adjacent Chinese coastal region are characterized by belts of deeply eroded high grade metamorphic rocks of Precambrian to Paleozoic age, which host younger granitoid-related mineral deposits formed at significant depth. In contrast, gold and silver mineralization in Koreas southeastern province occur in hydrothermal quartz veins that fill fracture zones in Cretaceous volcanic and sedimentary rocks of the Gyeongsang Basin, or in granites. Nearby southern Japan is well known for epithermal/hot spring gold-silver deposits associated with very late Tertiary silicic volcanic rocks and hot springs, but such young systems are not found in the Republic of Korea. In southeastern Korea the host rocks are older and the shallow environment has largely been removed by erosion. The predominant country rock of epithermal systems is weakly regionally-metamorphosed (albite-epidote to hornblende hornfels) sediments and igneous rocks. These rocks are cut by abundant areas of zoned pyrophyllite+sericite+kaolinite/dickite+alunite diaspore dumortierite alteration, and locally by epithermal precious and base metal veining which we discuss in this paper. All of the gold-silver deposits in the province are generally characterized as gold-silver or "silver-dominant" type deposits which contain more silver-bearing minerals than those deposits in central Korea (Choi *et al.*, 1994).

The Tongyeong mine lies near the southern edge of the town of Tongyeong, at Lat. 34° 50' 8", Long. 128° 26' 4". This epithermal deposit formed in proximity to Late Cretaceous granites and is characterized by relatively low Au/Ag ratios (1:10-1:200) and abundant and complex sulfide mineralization. It is unusual among the deposits of Korea, and the world as well, for an abundance of silver tellurides. The Au-Ag-Te vein mineralization of the deposit consists of two generations: 1) early, characterized by gold precipitation, and 2) late, represented by silver-rich or Te-bearing minerals. There are no preserved manifestations (paleosinters, etc) of hot springs. Ongoing detailed field work and laboratory alteration studies suggest that epithermal precious metal veining and nearby district-scale pyrophyllite kaolinite/dickite±sulfide alteration are separate events (Park and Choi, 1989; James *et al.*, 1999).

Mineralogical data on electrum-sphalerite and arsenopyrite geothermometry and fluid inclusions exists for various assemblages in this mine. These data indicate that the gold and silver mineralization occurred at temperatures of 190~280°C and 150~180°C, respectively (Choi *et al.*, 1994). These suggest that the gold-silver mineralization formed under low temperature and pressure (epithermal) conditions. These samples led Shelton *et al.* (1990) studied to the geochemically-derived conclusion that gold-silver deposition occurred at temperatures of <240°C in response to boiling and cooling at depths of <1.0 km. Shelton *et al.* documented the complex mineralogy, geochemistry, and water rock interactions in this shallow hydrothermal system.

In this paper we model quantitatively the controls of main-stage hydrothermal mineral deposition and mineral zoning pattern at Tongyeong, using chemical speciation and reaction path calculations. Our modeling draws on the detailed mineralogical and chemical framework established by Shelton *et al.* (1990), and thermodynamically-based modeling programs. Reed and Spycher (1985) modeled the results of boiling and acidification in a small epithermal ore system. Their chemical speciation and reaction path calculations used three steps: reaction with andesite, boiling, and dilution of metal bearing fluids and heated meteoric ground water. The main processes Reed and Spycher considered were the reaction of a single fluid with andesite host at 280°C, isobaric

cooling of that fluid from 260°C to 120°C, and boiling and mixing of that fluid with decreasing pressure and temperature. Reaction path studies on some similar aspects of the Acupan district, Philippines are presented by Cooke and McPhail (2001), and for low temperature lead zinc systems by Plumlee *et al.* (1994).

## 2. GEOLOGY AND ORE DEPOSITS

### 2.1. Geology

The Tongyeong mine area is near the present day southernmost exposure of the Cretaceous Gyeongsang Basin. Rocks of the basin belong mainly to the Gyeongsang Supergroup, consisting mainly of post orogenic, molasse-type sediments intercalated with lavas and volcaniclastic rocks. Strata of the Gyeongsang Supergroup dip at very low angles and rest unconformably on Precambrian metamorphic rocks of the Ryeongnam massif and upper Proterozoic metasediments of the Ogcheon Group. The Gyeongsang Supergroup is divided into three groups. The youngest of these, the Upper Cretaceous Yucheon Group, crops out in the mine area. It is a sequence of predominantly volcanic rocks that conformably overlies the Hayang and Sindong Groups. Three main units of the Yucheon Group are found in the mine area. They are, in ascending stratigraphic order: andesitic lapilli tuff, andesite, and the Jangpyeongri Formation (Fig. 1).

The lapilli tuff unit has an andesitic matrix with fragments of porphyritic andesite, aphanitic andesite, tuff, plagioclase grains, and small amounts of epidote, calcite, and iron oxides. The andesite unit occurs as both extrusive rocks and as intrusive bodies which commonly intrude the andesitic lapilli tuff. Overlying the andesitic lapilli tuff and andesite, the Jangpyeongri Formation is a mixed sequence of tuffaceous sandstone, tuffaceous con-

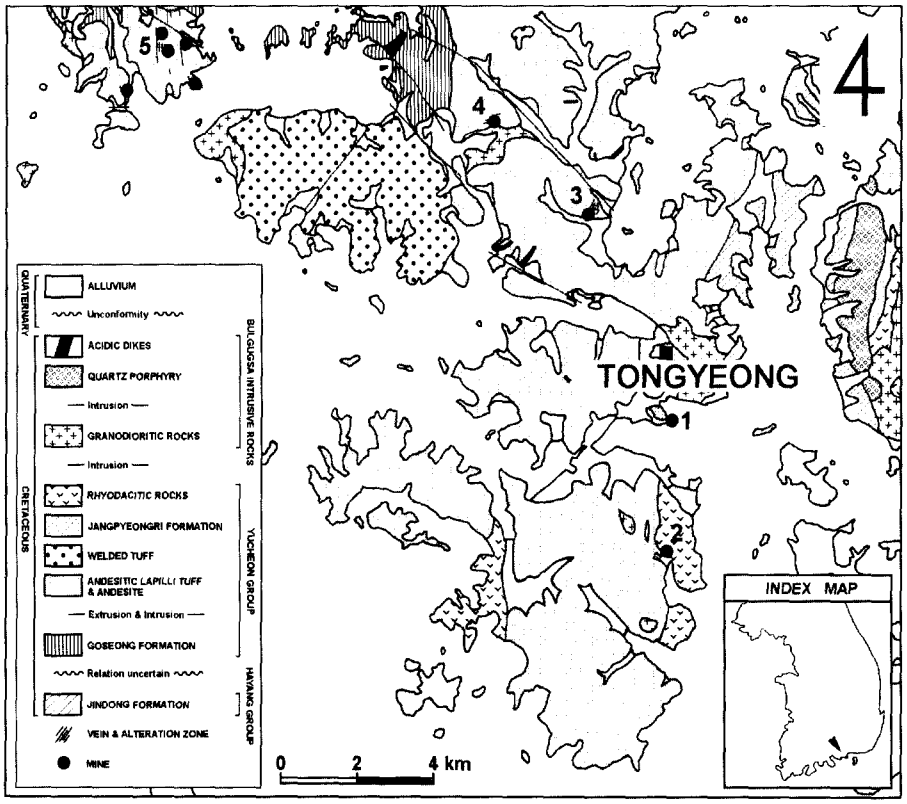


**Fig. 1.** Geological map of the study area and the location of mines. 1; Tongyeong (gold), 2; Mireugdo (pyrophyllite), 3; Kwangdo (pyrophyllite), 4; Bongsang (gold), 5; Goseong (copper).

glomerate, sandy shale, and shale. These subaqueous tuffaceous sedimentary rocks strike N15° to 30°E, dip 15° to 20°SE and show facies changes both laterally and vertically (Hwang, 1978). The calc-alkaline Bulgugsa Series rocks, mainly granodiorite, locally intrude the Yucheon Group in the mine area. The Bulgugsa rocks are Cretaceous orogenic andesites generated near the Asian continental margin. Local geology is described in several papers, e.g. Fletcher, 1976, Park (1983), Kim and Shin (1989), Shelton *et al.* (1990), James *et al.* (1999).

## 2.2. Ore deposits

The ore vein is well described by Park (1983), Kim and Shin (1989), and Shelton *et al.* (1990). Ore occurs along a steeply dipping hydrothermal quartz vein which formed by open-space filling of a fault plane in volcanic rocks of the Yucheon Group. The ore vein varies from 0.3 to 7.0 m in thickness (usually <1.2 m). It strikes N50° to 60°W, dips 70° to 80°SW, and extends >0.7 km along strike The Tongyeong mine produced more than 5 tonnes of gold 1916-1927. Based on history of the Japanese Colonial Era, later production data may be incomplete (only 1943-1945 records were found, and note only <200 kg Au). Where data exists, gold grades averaged 12 g/tonne, and silver 135 g/tonne. Grade and width extensively vary, hence some areas along the vein produced no ore. Recent assays show lower grade material was left unmined. The top of the system, of unknown extent, has been eroded away. Thus the full size of the system is not known. The vein shows a close spatial relationship to shallow-seated Bulgugsa granodiorite plutonism. The vein is frequently displaced by numerous, steeply dipping post ore faults striking N20° to N50°E. Horizontal displacements range from a few cm to >80 m. The ore body at Tongyeong is less than 800 m long and is faulted off at both ends. Workings and 1980s drilling tested mineralization to 250 m below the surface but failed to find high grade ore. The most extensive exploitation was on the 11$^{th}$ level. Twelve levels were developed, and Lee (1991) obtained some samples from top to bottom. The bulk of the material used in this study was from level 4. Within ore bodies the vein contains a higher percentage of wall-rock breccias. Ore shoots typically developed at points of vertical and horizontal bending of the vein.

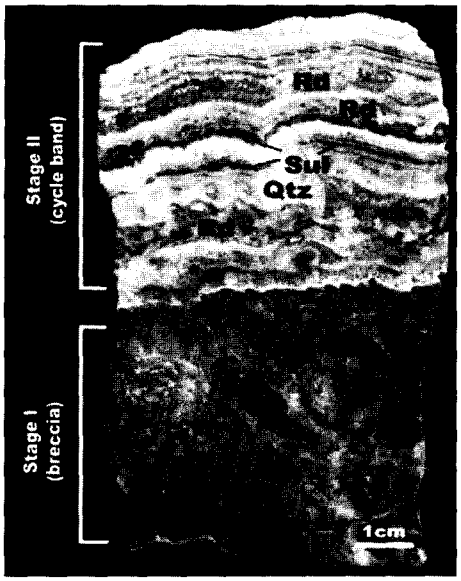


**Fig. 2.** A representative stratigraphy of the stage±veining in the Tongyeong Au-Ag-Te-bearing epithermal system. The boundaries of quartz (Qtz; white parts) bands and rhodochrosite (kutnahorite) bands are sharp. No primary pyrites occur in rhodochrosite (Rd), but some replaced pyrites (secondary) occur in rhodochrosite. Some rhodochrosite shows leaching texture at boundary of rhodochrosite band and sulfide (Sul) rich bands. Some illite is contained in pyrite rich band. Level nine, Tongyeong mine.

The ore vein consists mainly of multiple generations of breccias and bands with quartz, rhodochrosite, ankerite, calcite, base metal sulfides, gold, silver and telluride minerals. Chalcedonic quartz and rhodochrosite are rhythmically banded and colloform in texture throughout most of the vein (Fig. 2). Ore minerals occur as polymineralic bands ranging from 0.1 to 4.0 cm in width and also as disseminations in quartz. Sulfide bands with associated gold and silver minerals occur commonly at the contact between quartz and rhodochrosite bands. Lateral mineral zoning is commonly observed in the thickest ore bands. Vertical zoning of vein minerals is not evident, although pyrite, galena and sphalerite are more concentrated in the southern portion of the lower levels of the mine (Shelton *et al.*, 1990).

## 3. MINERALOGY AND PARAGENESIS

Four main stages have been distinguished based on structure and mineral assemblages. StageI is an early breccia filling and StageII contains the Au-Ag ores, while later stagesIII and IV are barren (Table 1). Areas of the vein occupied by StageI are highly brecciated and occur as discontinuous segments (<15) cm thick found mainly at the contact between wall rock and stageII veins and as inclusions in late vein stages. StageI contains mostly quartz and minor pyrite, and matrix in StageI breccias is altered to illite/smectite, hematite and quartz (Fig. 2). StageII vein matter, in places 2 m thick, occurs frequently as matrix cementing highly brecciated fragments of stageand wall rock. It is cut by numerous later thin quartz veins. The ore mineral assemblages and associated gangue phases in stageII can be clearly divided into two general associations: an early cycle (band) that included the introduction of most of the sulfides and electrum, and a later cycle in which base metal and carbonate bearing assemblage (mostly rhodochrosite) became dominant (Fig. 3). Tellurides and some electrum occur as small rounded grains within sub-to euhedral pyrite or anhedral galena in stageII. StageII volumetrically dominates mineralization, and consists mainly of gray to clear quartz, carbonates, sulfides, electrum, and tellurides. StageII is composed of several rhythmical band which show a progressive change in ore mineralogy with increasing paragenetic time (Shelton *et al.*, 1990): electrum→electrum+argentite→electrum + Ag tellurides→Ag tellurides+native silver.

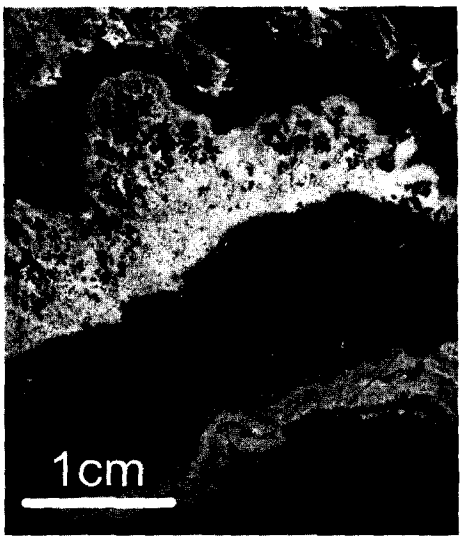


**Fig. 3.** Photomicrograph of vein textures of the alternating quartz (white) and rhodochrosite bands (gray) with disseminated sulfides (black). Level nine, Tongyeong mine.

Early electrum in stageII has a lower Ag content (36.7-40.9 wt.% Ag) than later bands of electrum (46.4-52.1 wt.% Ag; Table 2 and 3).

StagesIII and IV contain mainly milky quartz, minor rhodochrosite and calcite, and rare sulfides. The most common types of wall-rock alteration associated with the vein are argillic, propylitic, silicic, and sericitic. This alteration, characterized by illite, sericite, and fine-grained silica, is intimately associated with stageI mineralization. Reddish-brown jasperoid occurs as breccia fragments in strongly sericitized alteration selvages adjacent to quartz veins. Advanced argillic alteration (Woit-

**Table 1.** Representative stratigraphic units of a vein, and its inferred genesis and history.

| Stage | Unit | Inferences and history | Inferred cause |
|---|---|---|---|
| Alteration | illite/smectite and pyrite | relatively acid | water-rock interaction |
| StageI<br>(breccia) | breccia and gray quartz<br>hematite and quartz | physical break-up opened up<br>excess heat boiling intrusion of $O_2$-bearing water | break<br>boil and quench |
| StageII*<br>(cyclic band) | rhodochrosite<br>fine-grained sulfides and native silver<br>course-grained sulfides and native silver<br>clear comb quartz | boiling and pH increase<br>rapid deposition<br>excess heat boiling<br>quartz saturated by temperature effect | boil<br>quench and dilute<br>boil<br>quiescent time |
| StageIII<br>(cross cutting vein) | milky quartz<br>clear quartz | excess heat boiling<br>quartz saturated by temperature effect | boil<br>quiescent time |
| StageIV | calcite | ground water heating | heating without boil |

*Cyclic bands of the stageII vein indicate some fundamental processes are repeated. Electrum is associated with sulfides of the stageII.

**Table 2.** EPMA analysis of electrum from stageII of the Tongyeong Au-Ag-Te mine.

| Specimen No. | | Weight percent | | | Atomic percent | | |
|---|---|---|---|---|---|---|---|
| | | Ag | Au | Sum | Ag | Au | Ag/Au |
| Early | TE-1 | 36.74 | 61.24 | 97.98 | 52.3 | 47.7 | 1.10 |
| | TE-2 | 37.59 | 61.25 | 98.84 | 52.8 | 47.2 | 1.12 |
| | TE-3 | 37.60 | 59.76 | 97.36 | 53.5 | 46.5 | 1.15 |
| | TE-4 | 37.55 | 61.16 | 98.71 | 52.9 | 47.1 | 1.12 |
| | TE-5 | 36.32 | 62.31 | 98.63 | 51.6 | 48.4 | 1.07 |
| | TE-6 | 40.93 | 57.60 | 98.53 | 56.5 | 43.5 | 1.30 |
| Late | TLA-1 | 50.70 | 47.10 | 97.80 | 66.3 | 33.7 | 1.97 |
| | TLB-2 | 49.84 | 48.40 | 98.24 | 65.3 | 34.7 | 1.88 |
| | TL1-1 | 49.97 | 46.36 | 96.33 | 66.3 | 33.7 | 1.97 |
| | TL1-2 | 46.49 | 52.05 | 98.54 | 62.0 | 38.0 | 1.63 |

**Table 3.** Microprobe analyses of pyrites from the Tongyeong epithermal veins.

| Sample No. | Fe | Zn | Mn | Cd | As | Sb | Ag | Stage |
|---|---|---|---|---|---|---|---|---|
| Level 5 | | | | | | | | |
| 2-D | 32.808 | - | 0.013 | 0.032 | 0.125 | - | - | II |
| 10-D | 32.682 | 0.129 | 0.073 | - | - | - | - | II |
| 3-E | 32.742 | - | 0.102 | - | - | 0.042 | 0.100 | II |
| Level 9 | | | | | | | | |
| 1-A | 32.262 | 0.161 | 0.065 | - | 0.051 | - | 0.010 | I |
| 1-B | 32.258 | 0.051 | - | - | 0.489 | 0.033 | - | I |
| 3-C | 33.193 | 0.018 | 0.016 | - | 0.388 | - | - | I |
| 3-A | 32.695 | - | - | 0.054 | 0.519 | 0.028 | 0.121 | II |
| 3-B | 32.541 | - | - | - | 0.992 | - | - | II |
| Level 12 | | | | | | | | |
| A | 32.604 | 0.075 | 0.093 | 0.088 | 0.136 | - | 0.082 | II |
| B | 32.737 | - | - | 0.030 | 0.085 | - | 0.024 | II |
| C | 33.015 | 0.118 | - | 0.024 | 0.971 | - | 0.170 | II |
| D | 32.804 | - | - | - | 0.243 | - | - | II |
| E | 32.564 | 0.038 | 0.043 | - | 0.166 | - | 0.045 | II |

*-; not detected

sekhowskaya and Hemley, 1995) is lacking within this epithermal vein deposit. However, within 2 km of the mine, pyrophyllite quarries contain wide zones and pods of advanced argillic alteration (Fletcher, 1976), locally containing minor sulfides. These most probably are an end member of unrelated high level hydrothermal processes, in which heat related to shallow pluton emplacement generated regional low temperature fluids. These became supersaturated with silica, generating pyrophyllite in permeable zones at shallow depths (James *et al.*, 1999).

Pyrite at Tongyeong is associated closely in time with gold mineralization. Some of the ore-stage (stageII) pyrite is As-rich. Most electrum was deposited late in the precipitation of relatively arsenic rich pyrites in stageII. Arsenic concentrations in pyrite are shown in Table 3.

## 4. GEOCHEMICAL BACKGROUND

### 4.1. Host rock

Fresh and weakly altered host andesites (Fig. 4) were analysed (Table 4). The altered andesites are characteristically more enriched in K (hydrothermally altered andesites-TY 7 and TY 10) than relatively fresh rock (TY 1). The difference between the samples is consistent with, the decrease of Ca and increase in K (Table 4). Only Cu appears to be anomalous in the host rock. Pb, Sb, Te, As, Hg,

**Table 4.** Representative compositions of andesite in Tongyeong area.

| Elements | TY-1 | TY-7 | TY-10 |
|---|---|---|---|
| $SiO_2$(wt %) | 53.86 | 55.25 | 54.28 |
| $Al_2O_3$ | 16.53 | 16.32 | 15.16 |
| $Fe_2O_3$* | 8.18 | 6.49 | 7.74 |
| $TiO_2$ | 0.86 | 0.86 | 0.76 |
| MnO | 0.14 | 0.11 | 0.92 |
| CaO | 8.77 | 5.07 | 2.20 |
| MgO | 4.66 | 2.26 | 4.69 |
| $K_2O$ | 1.34 | 2.65 | 8.49 |
| $Na_2O$ | 2.16 | 3.37 | 0.11 |
| $P_2O_5$ | 0.23 | 0.22 | 0.22 |
| LOI | 2.51 | 6.52 | 4.10 |
| Total | 99.23 | 99.12 | 98.65 |
| Zn (ppm) | 88.79 | 79.52 | 69.79 |
| Pb, Sb, Te, As, Hg, Ag** | n.d. | n.d. | n.d. |
| Cu | 98.65 | 79.52 | 58.33 |
| Ba | 226.90 | 1391.68 | 2323.17 |

Remark: All samples were analyzed three times and averaged. $Fe_2O_3$*=Total Fe, LOI = Loss of Ignition. **: n.d. = Not determined due low concentrations below detection limit (<0.1 ppm). Analyses by Center for Mineral Resource Studies (CMR), Korea University, by X-ray fluorescence except as noted.

and Ag were not detected in the andesitic host (detection limits are <0.1 ppm). Ba shows higher content in altered host rock, but Cu and Zn decrease in altered host rock. In vein ores, measured Au concentrations range from <0.1 ppm (detection limit) to 120 ppm and Ag values range from <0.2 ppm (detection limit) to 860 ppm in mine production. There is a strong positive correlation between Au and Ag.

Geochemical environment of ore deposition: Shelton *et al.*, (1990) concluded the formation of the Tongyeong Au-Ag-Te deposits resulted from a convective hydrothermal system recharged by meteoric water. They infer a history of progressive cooling and dilution of ore-forming solution from the linear relationship between homogenization temperatures and salinities of fluid inclusion. They also reported that only liquid-rich fluid inclusions and no definitive boiling evidences were observed. We identified many very small single-phase inclusions, both liquid-only, and apparent vapor-only inclusion distributed in chalcedonic quartz bands of stageII (Fig. 5). The mineralogy reflects rapid decreases in temperature and fugacity of sulfur, with dilution by groundwater into the system (Reed and Spycher, 1985; Park *et al.*, 1992). Also fluid inclusion data (Shelton *et al.*, 1990; Lee, 1991) indicate repeated cooling and dilution of ore fluids. A similar mixing trend is also apparent in hydrogen and oxygen isotopic data (Shelton *et al.*, 1990). We use these results to reconstruct the ore forming solution. Homogenization and electrum-sphalerite temperatures of the ore-forming stage range from 180-260°C with mean of approximately 220°C (Table 5). The salinities range from 1~3 equiv. wt.% NaCl. Homogenization temperatures of primary fluid inclusions in quartz are generally lower than temperatures determined from mineral phase relations and compositions. Part of this temperature difference could have been due to quartz deposition at consistently lower temperatures than sulfides and electrum. Alter-

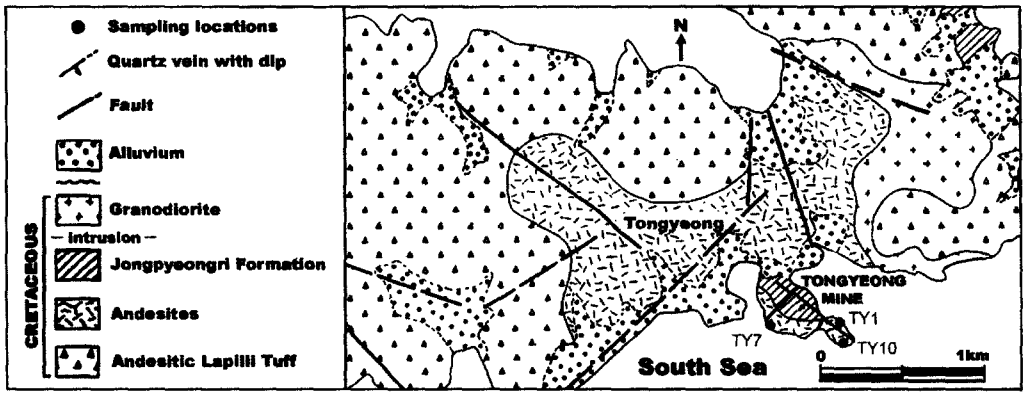


**Fig. 4.** Sample location map of host andesite analysed in this study (after Shelton *et al.*, 1990).

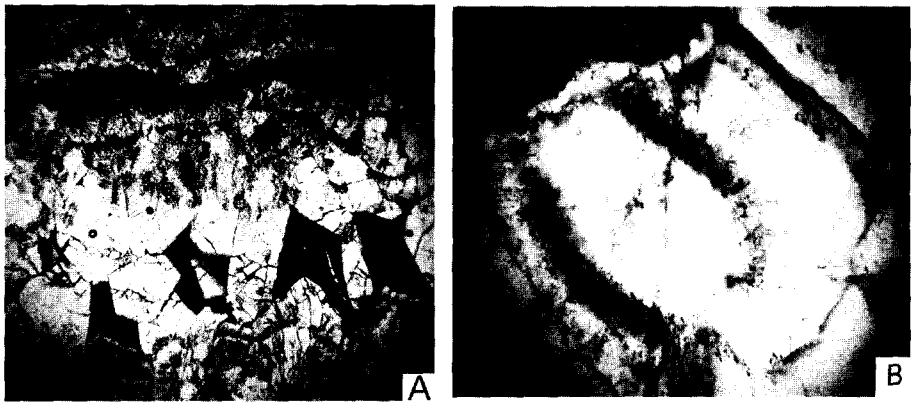


**Fig. 5.** A: Photomicrograph showing vein associations with quartz, and rhodochrosite and sulfides. B: Zoned quartz showing different density of fluid inclusions due to repeated boiling and mixing. Level twelve, Tongyeong mine.

natively, the difference between homogenization and mineral assemblage temperatures could be real and reflect a pressure correction for the fluid inclusions. Using the data of Potter (1977) for volumetric properties of the system $H_2O$-NaCl, a temperature correction of 25°C for a 6 wt percent NaCl fluid at a homogenization temperature of 260°C corresponds to a pressure of approximately 300 bars. The same determination for a 1 wt percent NaCl fluids at 170°Ccorresponds to a pressure of approximately 225 bars. The logarithms of total sulfur concentration range from 2 to 3 moles. Stable isotope compositions of mineralizing fluids from Tongyeong (D=-44 to -61; $\delta^{18}O$=-6.8 to 9.4) are similar to modern meteoric and thermal spring waters in the area and indicate meteoric water dominance during all stages of the Au-Ag-Te mineralizing system (Shelton *et al.*, 1990).

To reconstruct the ore-forming solution, information from fluid inclusion data was augmented by several assumptions. We propose a combination of extensive boiling and mixing processes in the Tongyeong system which resulted in the entrapment of co-existing fluids with variable salinities at the same time. The hydrothermal fluid rose along fractures under hydrostatic conditions, and reached the boiling isotherm level for the fluid. Boiling and mixing of hydrothermal solutions commonly occur in present geothermal systems and are often cited as ore-forming processes in epithermal deposits (e.g. Buchanan 1981; Heald *et al.* 1987). General aspects of the physicochemical changes attending boiling in epithermal systems have modeled previously (Drummond and Ohmoto 1985; Reed and Spycher 1985; Cline *et al.* 1992). Roedder (1960) proposed variable liquid/vapor ratios in contemporaneous fluid inclusion which had been trapped various amounts of liquid and vapor phase. Direct fluid inclusion evidence for boiling at Tongyeong is observed in stage (Fig. 5)

Some indirect evidence for boiling has also been found. Illite/smectite alteration is well developed in stageI breccias which are interpreted to have formed by the reaction of the andesitic rocks with acid species derived from hydrothermal fluids during boiling. Repeated carbonate (dominantly rhodochrosite) bands in stageII indicate deposition by sporadic boiling. Fine-grained milky quartz overgrown on clear quartz shows a zoned texture (Fig. 5).

Fluid inclusion studies are interpreted as follows: low salinity inclusions represent the composition of the liquid phase after mixing, and the moderate salinity inclusions are representative of the early liquid phase, before boiling and vapor loss in an open system. This mechanism resulted in the entrapment of fluids with variable salinities at the same time. Deposition of ore minerals within the Tongyeong vein system also occurred at this time as a result of boiling and gas loss. Fluid inclusion data of stageII quartz indicate the homogenization temperatures and salinities decreased progressively. Although Shelton *et al.* (1990) did not analyses inclusions formed by boiling condition, we observed many high salinity inclusions with halite daughters of very small size (<2 μm). This

is evidence that mixing of the hydrothermal fluid with overlying groundwater was the dominant ore deposition mechanism of stageII in the Tongyeong vein system. We conclude fluid inclusion data indicate mixing between hydrothermal fluids and overlying dilute heated groundwater and cool groundwater.

Boiling is an important process in gold precipitation within low-sulfidation epithermal systems (Hedenquist and Henley, 1985; Drummond and Ohmoto, 1985; Larson and Taylor, 1987) as $H_2S$, the principal species for gold transport (Seward, 1973) is lost into the vapor phase. Boiling also releases $CO_2$ to the vapor, resulting in an increase in solution pH, shifting from illite to adularia stability, and leading to the precipitation of calcite and adularia (e.g., Browne and Ellis, 1970). From equilibrium thermodynamics studies, the minus logarithms of fugacity of $O_2$, $CO_2$, and $S_2$ on stageII are 12.5~-11, 0 to 5 and 38.6 to 34.4 respectively (Shelton *et al.*, 1990). Multiple cyclic bands of rhodochrosite in the Tongyeong vein also indicate releases of $CO_2$ gas by boiling (Fig. 2).

### 4.2. Methods of calculation

The chemical speciation and reaction path calculations were accomplished with the multicomponent heterogeneous equilibrium programs SOLVEQ and CHILLER (Reed, 1982). The speciation program SOLVEQ was used to calculate starting compositions for the fluids used for the reaction path calculations. The reaction path program CHILLER models change in fluid chemistry and amounts of minerals precipitated from solution. This program was used to calculate each series of steps over various chemical evolution paths such as boiling, cooling, fluid mixing, and titration reaction.

Thermodyamic data used in the present calculations are contained within the SOLTHERM database, with data for solids and gases from the SUPCRT database (Johnson *et al,* 1992), and data for aqueous species from sources listed in SOLTHERM. Some modifications were made to the CHILLER and SOLVEQ database during the course of calculation. Activity coefficients were calculated using the method derived by Helgeson *et al.* (1981) and they were determined to be valid for ionic strengths of Tongyeong hydrothermal fluids. Calculated ionic strength of the Tongyeong ore fluid is at the upper limits of reliability of the activity coefficient.

When simulating boiling, CHILLER is used to solve for the amount and composition of the aqueous, solid, and, gas phases at equilibrium and the pressure at which gas and liquid are in such proportions that the sum of their respective heat contents equals a given total enthalpy plus an optional heat gain or loss for the system. There are accomplished by solving simultaneously a set of mass balance and mass action equations and an enthalpy equation. The amount of each gas species in equilibrium with the aqueous phase is dictated by mass balance and mass action equations that are similar in form to the equations used for mineral solid solution (Reed, 1982). Mass action equations for gases make use of true equilibrium constants. These are different from Henry's law constants, $K_h$, in being independent of salinity and defined for a given specific chemical reaction. Most of the speciation and reaction path calculations were made assuming that equilibrium was attained between sulfate and sulfide in solution.

In this study, multicomponent heterogeneous chemical equilibrium computations are used to simulate the transportation and deposition of base metals and precious metals in a boiling and simple cooling epithermal system. The main processes considered were (1) the reaction of a single fluid with andesitic rock host at 280°C, (2) the boiling of parent liquid 260°C to 120°C, and (3) the cooling with mixing of fluid with both decreasing pressure and temperature from 260°C to 120°C; also gas extraction at 200°C, (4) steam heated 260°C

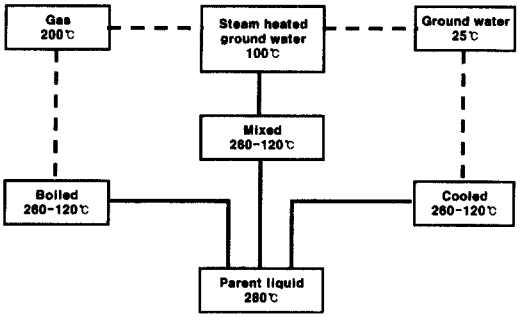


**Fig. 6.** Schematic diagram showing the relationship of the reaction path models of the Tongyeong epithermal system.

groundwater cooling to 150°C. Flow diagrams of the calculations presented in this study are shown in Fig. 6.

## 5. STARTING COMPOSITION OF FLUIDS

### 5.1. Parent fluid

The composition used in this study is a Broadlands-type water (Reed and Spycher, 1985). The initial composition and chemical speciation of the ore fluids used in the reaction path calculations were calculated with SOLVEQ, using measured fluid inclusion temperature, salinities and assuming saturation with various hydrothermal minerals (Table 5). These initial fluid compositions were used as input for CHILLER. For a closed system model, the amounts of andesite (composition based on petrographic data) and fluid were held constant. The entire amount of fluid reacts with progressively larger amounts of rock. Temperatures and salinities for the fluids were based on fluid inclusion measurements on stageII veins. Dissolved species were calculated using SOLVEQ by assuming the solution was in equilibrium with the following vein minerals: muscovite (source for dissolved Al), native gold (Au), pyrite (Fe), Chalcopyrite (Cu), acanthite (Ag), rhodochrosite (Mn), and quartz ($SiO_{2(aq)}$). In addition, Ca content was chosen to result in a fluid that is unsaturated with respect to calcite by approximately 1 log unit (to be consistent with the lack of calcite in the ore stage). We used calculated minimum values for the dissolved species because the solution may have been supersaturated with respect to the phase precipitated. In the case of silica quartz was chosen to control the dissolved silica content, as it is the more soluble phase. In reality, the dissolved silica content could have been significant higher, given the kinetic inhibition of quartz precipitation at temperatures <250°C (Fournier, 1985). Total Cl in solution was calculated by SOLVEQ by charge balance; this is reasonable, given that the total calculated chloride values generally are close to the charge sum for Na, K, and Ca. The reconstructed fluid is similar in composition to the geothermal water modeling by Spycher and Reed (1989) and Saunders and Schoenly (1995) except for telluride composition. The ore-forming solution has 200 ppb Au, which is the saturation value at 260°C, pH=5.9, and -3 to 2 moles of log total sulfur dissolved. The pH chosen for the model solution was based on the minimum stability of muscovite and rhodochrosite.

The early fluid composition used for alteration reaction in the modeling is relatively acidic and equilibrium with sericite, quartz and pyrite at 280°C and cooled to 260°C. The second and third stage fluid was taken from the former titrated fluid and then saturated with pyrite, chalcopyrite, galena and sphalerite. These assumed mineral saturation values were chosen based on ore minerals. Thus, it is possible to compare meaningfully the modeling result with a real geologic example.

### 5.2. Overlying groundwaters

Chemical constraints on overlying steam heated groundwaters are limited. As a result, a variety of ground-water compositions were tried in the calculations. The composition used most frequently, near that of a steam-heated groundwater (containing $CO^2$, $SO_4^{2-}$, $H_2S$, and other species derived from gas condensates) from the Tauhara geothermal system (Reed, 1992), is listed in Table 5. Modifications of this composition were used in some runs to test for the effects on the predicted mineral precipitation sequence of variations in the pH, oxidation state, sulfidation state, iron, aluminum, and silica contents, and temperature of the ground water.

**Table 5.** Silver content of electrum, iron content of sphalerite, electrum-sphalerite temperatures and filling temperatures of fluid inclusions from the Tongyeong epithermal Au-Ag-Te deposit.

| Stage | Ag content of electrum (atm. fraction) (No. analyses, avg.) | Iron content of sphalerite (FeS mole %) (No. analyses, avg.) | Electrum-sphalerite temperature* (°C) (min., avg., max.) | | Filling temperature (°C) (avg.) |
|---|---|---|---|---|---|
| | | | I | II | |
| Early | 0.516-0.565(6, 0.533) | 1.66-6.42(8, 3.76) | 253, 273, 282 | 233, 256, 265 | 226 |
| Late | 0.620-0.663(4, 0.650) | 3.33-4.53(7, 3.84) | 250, 251, 253 | 230, 231, 232 | 186 |

*Calculated using Electrum-sphalerite temperature equations (6) and (7) from Shikazono (1985), respectively

## 6. REACTION PATH MODELING

Reaction path models are a simplification of natural processes, which here simulates fluid from the Tongyeong epithermal system. They describe chemical processes that can approximate ore deposition. Au-Ag-Te precipitation closely compares to the result of repeated boiling and ground water mixing. Natural geothermal fluids do actually equilibrate with their wall rocks, as can be shown by whole-system geothermometry using graphs of mineral saturation indices vs. temperature for reconstructed fluids from may system (Reed and Spycher, 1984). Equilibration with wall rock does not mean that the fluid reaches complete equilibrium with the primary minerals of the host rock, but overall equilibrium between fluid and rock has been achieved. The formation of wall-rock alteration was simulated by calculating the reaction of andesite at 150 bars and 280°C, that was initially saturated with quartz, muscovite, Mg and Fe chlorite, pyrite, chalcopyrite, galena, sphalerite, electrum, and telluride minerals. The chemical composition, oxidation, state and pH of hydrothermal fluid are fixed by reaction of the fluid with wall rock. Once the hydrothermal wall rock reaction fixes pH, it determines the type of reaction paths. The calculations are divided into named segments (simple cooling, boiling and mixing) in fig. 5. In an andesite reaction with an assumed fluid, pH is gradually increased and quartz, sericite, chlorite and pyrite precipitate with decreasing water/rock ratio.

Simple Cooling Reaction Path: Cooling of the hydrothermal fluid could have occurred due to conductive heat loss as the fluids moved into cooler rocks. Reaction path cooling of a single fluid without boiling predicts the precipitation of vein minerals (Fig. 7). Quartz, pyrite, chalcopyrite, sphalerite, calaverite precipitated at high temperature, and muscovite, hessite, sphalerite, galena, and acanthite at low temperature. In this numerical experiment, quartz and pyrite precipitate immediately at high temperature and are followed after a few degrees temperature drop by pyrite, chalcopyrite, sphalerite, galena, and acanthite (Fig. 6). But no electrum is precipitated by cooling alone. Kaolinite is replaced by muscovite at 200°C. The activity of $H^+$ initially increase but this trend reverses as $HSO_4$ forms with decreasing temperature. When the hydrothermal fluid cools without addition of cool groundwater, $HSO_4^-$ dissociates to $H^+$ and $SO_4^{2-}$ with decreasing temperature. Precipitation of the sulfide assemblage in the cooling-only numerical experiment clearly is not the principal cause of electrum precipitation.

Boiling Reaction Path: Boiling and consequent cooling result in precipitation of vein minerals,

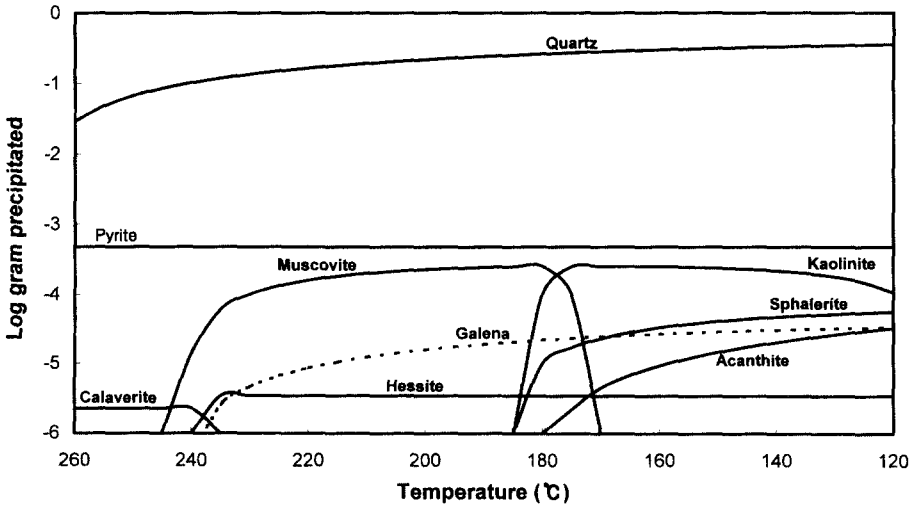


**Fig. 7.** Reaction path diagram showing amounts of mineral precipitated during cooling of the assumed stageII fluid from 260° to 120°C.

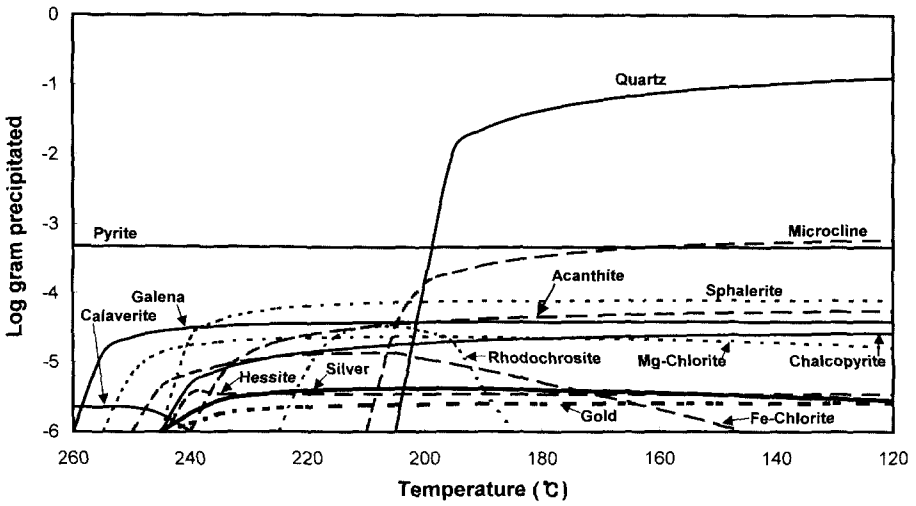


**Fig. 8.** Reaction path diagram showing amounts of mineral precipited during boiling of the assumed stageII fluid from 260° to 120°C.

which fractionate as the liquid and gas ascends. The gas and liquid are assumed to remain in contact with each other throughout ascent. The chemical system is treated as partially open because minerals are removed as they form. The computed scale mineral assemblage is thermodynamically quite stable (Reed, 1985). In a boiling geothermal system, the temperature profile in the boiling zone matches the P-T path of boiling water (isoenthapic). When a homogeneous aqueous phase rises in a hydrothermal system, it experiences a decrease in pressure. The resultant boiling induces a temperature decrease and a pH increase, which cause minerals to precipitate. Thus, the initially homogeneous aqueous phase separates into several phases including gas, liquid, and minerals. An open-system boiling process (gas removed from the hydrothermal fluids at each reaction step) was modeled.

Hydrothermal fluids with assumed initial compositions initially matching Tongyeong fluids (Table 5) immediately become undersaturated with respect to most sulfides during boiling. Boiling of stageII fluids precipitates quartz, Mg- and Fe-chlorite, pyrite, chalcopyrite, galena, sphalerite, acanthite, calaverite, hessite and electrum (Fig. 8). The lack of sulfide precipitation at relatively high temperature results from low reduced sulfur ($HS^-$) contents of fluid. The initial boiling of fluid at about 260 deposits quartz, pyrite, Mg and Fe chlorite, chalcopyrite and calaverite. After a 10 temperature drop, the fluids becomes undersaturated with sphalerite, galena, acanthite, hessite and electrum (Fig. 8). With temperature drop by continuous boiling, the fluid becomes undersaturated in chlorite and pyrite. Starting at 260°C, the liquid water (Table 6) has a pH of 6.17 and solids are undersaturated or exactly saturated except for quartz and pyrite. The pH increases at 120°C, driven by escape of $CO_2$ to a gas phase upon boiling. The pH increase is steep intially, as aqueous $CO_2$ is more strongly partitioned into the gas at the beginning of boiling than subsequently. The steep pH increase promotes precipitation of sulfides by boiling processes (Fig. 8). The temperature decrease combines with the pH increase to force sulfide and carbonate (rhodochrosite) precipitation.

As boiling proceeds between 227°C and 184°C, the precipitated assemblage is dominantly base metal sulfides and rhodochrosite. At 240°C and 227°C, microcline and acanthite precipitate respectively. Chlorite (Mg-Fe solid solution) precipitates near 250°C, with Mg content of chlorite increasing with temperature drop. Over the short temperature interval (270°C to 184°C) where the greatest mineral mass precipitates, the loss of reduced gases, $H_2$ and $CH_4$, causes oxidation of aqueous sulfide to sulfate, increasing sulfate molality. Degassing causes total aqueous carbonate and sulfide ($CO_3$ and HS) to decrease. This precipitation sequence

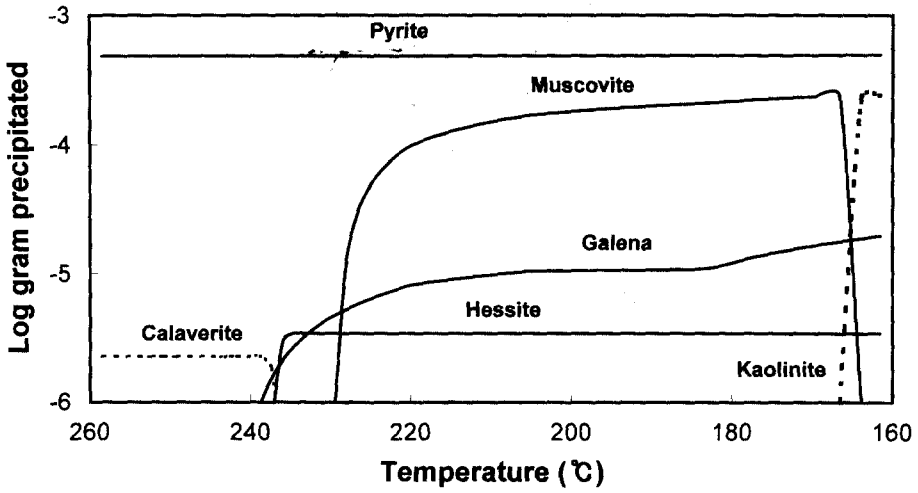


**Fig. 9.** Reaction path diagram showing amounts of mineral precipitated during mixing of the assumed stageII fluid with heated groundwater from 260° to 160°C.

closely resembles that at Tongyeong for the sulfide cycles in the

stageII assemblage. It is apparent that progressive boiling alone of the initial fluid in the Tongyeong environment could not have produced the complete stageII mineral zoning (band) patterns (e.g., Fig. 2).

### 6.2. Fluid mixing reaction path

Fluid inclusion study indicates relatively small variation (1 to 3 wt % NaCl) in salinity during the low temperature mineral deposition in the Tongyeong epithermal system. The fluid mixing path modeled in this study was carried out assuming isoentalpic conditions, with no heat loss to the wall rocks. A given mixing path tracks the progressive dilution of 1 kg of hydrothermal fluid by successive increments of ground water. Cooling and dilution accompanying mixing are important processes driving fluid chemistry evolution and mineral deposition, and cause breakdown of metal chloride complexes and the resulting precipitation of base metal sulfides, Te-bearing minerals, muscovite and kaolinite. The pH initially drops because hydrogen ions are released during sulfide precipitation, and then increases slightly because of the overriding effects of the higher pH ground water. Total reduced sulfur concentration in the hydrothermal fluids is initially low and decreases substantially during the mixing as a result of oxidation and sulfide precipitation. The hydrothermal fluid lacks sufficient reduced sulfur to precipitation both galena and sphalerite (Fig. 9). It does not produce electrum. Only a restricted range (260° to 150°C) of inmixed heated groundwater fluid composition produced very minor amounts of Te-bearing assemblages (Fig. 9). Therefore, mixing of different fluids is not an efficient gold precipitation mechanism in stageII.

## 7. CONCLUSIONS

Using calculation of simultaneous, multi-phase chemical equilibria, we identify chemical speciation and reaction paths that model fluid chemistry evolution and ore deposition in the Tongyeong epithermal system. A mineralogical and geochemical framework for Au-Ag-Te mineralization, established by previous researchers, was used to reconstruct the fluids. The main processes considered were reaction of a single fluid with an andesite host at 280°C, isobaric cooling of a single fluid from 260°C to 120°C, and boiling and mixing of fluid with both decreasing pressure and temperature. Reaction path modeling indicates that the main stage of Au-Ag-Te mineralization (stageII) resulted from boiling. The assemblages resulting from mixing include only small amounts of base metal sulfides with no electrum. The abundance of gold depends critically on the ratio of total base metals and iron to sulfide in the aqueous phase

**Table 6.** Temperature, saturation pressures and reference compositions of fluids used in reaction path calculations. (log values for gas phases.)

| Fluid | Hydrothermal fluids | | Ground water | |
|---|---|---|---|---|
| | parent brine | stage (II) | steam heated | cold |
| Temperature (°C) | 280 | 250~150 | 100 | 25 |
| Saturation pressure (bars) | 82.9522 | 66.6323 | - | 1 |
| pH | 6.43 | 6.17 | 5.7 | 7 |
| Total Cl *(m)* | .2749089E-01 | .2749089E-01 | 2.20E-03 | 7.33E-03 |
| Total $S_{OX}$ *(m)* | -.4257701E-02 | -.4257708E-02 | 1.10E-03 | 3.23E-03 |
| Total $CO_2$ *(m)* | - | - | 2.50E-03 | 2.02E-01 |
| Total $O_2$ *(m)* | - | - | - | 2.50E-02 |
| Total $S_{red}$ *(m)* | .9985828E-02 | .9985820E-02 | 2.00E-05 | - |
| Total $SiO_2$ *(m)* | .3036205E-02 | .3036205E-02 | 8.10E-04 | 1.05E-01 |
| Total Al *(m)* | .2253680E-05 | .2253680E-05 | - | 1.11E-05 |
| Total Ca *(m)* | .1561400E-04 | .1561400E-04 | 4.10E-04 | 7.24E-03 |
| Total Mg *(m)* | .2355503E-06 | .2355503E-06 | 1.00E-07 | 5.35E-03 |
| Total Fe *(m)* | .1180087E-07 | .4020242E-08 | 5.00E-10 | 1.79E-05 |
| Total K *(m)* | .3715700E-02 | .3715700E-02 | 9.70E-04 | 3.58E-03 |
| Total Na *(m)* | .2963300E-01 | .2963300E-01 | 3.00E-03 | 4.57E-03 |
| Total Mn *(m)* | .4140424E-05 | .4140424E-05 | - | - |
| Total Zn *(m)* | .8030000E-06 | .8030000E-06 | - | - |
| Total Cu *(m)* | .1126191E-06 | .1559973E-06 | - | - |
| Total Pb *(m)* | .1610000E-06 | .1610000E-06 | - | - |
| Total Ag *(m)* | .5000000E-06 | .5000000E-06 | - | - |
| Total Au *(m)* | .8010000E-08 | .8010003E-08 | - | - |
| Total Te *(m)* | .9596672E-16 | .6084875E-14 | - | - |
| Total F *(m)* | .2439100E-03 | .2439100E-03 | - | 1.74E-03 |
| gas phase | | | | |
| $fS_2$ | -11.501 | -13~-15 | -11.635 | - |
| $fCO_2$ | 1.107 | 0~+5 | 1.153 | - |
| $fO_2$ | -35.5 | -36~-39 | -37.092 | - |
| Salinity (eq. wt % NaCl) | 4~6 | 1~3 | - | - |

because gold is transported as an $Au(HS)_2$ complex, which is sensitive to sulfide activity. Thus boiling and mixing produce distinctly different mineralogy. Relatively large amounts of galena precipitate with a low degree of mixing, but sphalerite and acanthite contents increase with a high degree of mixing. Mineral assemblages and mineral zoning patterns (cyclic bands) are most likely to form from boiling, plus mixing of hydrothermal fluids with heated groundwater. The calculation for boiling yields mineral assemblages with large amounts of base metal and Au-Ag-Te mineralization.

Reaction path calculations are useful in explaining mineralogical variations. These can be useful guides to ore zone with in Au-Ag-Te-bearing epithermal systems that are meteoric water dominant. Also the modeling results provide useful tools for epithermal gold exploration in environments that are strongly influenced by shallow hydrologic processes such as boiling and fluid mixing. As gold behaves slightly differently from silver, base metals and tellurium, low-level metal zoning identified by simple rock-chip sampling (especially in zones with evidence of steam-heated groundwater) may suggest concealed locales of mixing and boiling (gold precipitation) at depth. Data can be plotted on geologic sections to identify permeable zone or structures. Successful application of Hg and Sb zoning in discovery of gold zones in epithermal/fossil geothermal systems (without the aid of numerical modeling) are well known in the

western U.S. Refinements using our modeling technique, perhaps incorporating other recent work on epithermal telluride precious metal systems (Cooke and McPhail, 2001) and argillic alteration systems in fractured rock (Xu and Pruess, 2001), published after our study was completed, may lead to further refinement of specific drilling targets.

## ACKNOWLEDGMENTS

This research was supported by Korea Research Foundation Grant (KRF-99-041-D00421 to M.E. Park). Parks underground sampling in 1982 and 1987 was assisted by mine staff. Jame's sampling in 1990 was assisted by C. Hamilton. Jamess present stay in Korea was funded by the Korea Federation of Science and Technology Societies. Collaboration with Mark H. Reed of the University of Oregon over many years is gratefully acknowledged.

## REFERENCES

Browne, P.R.L, Ellis, A.J. (1970) The Ohaki-Broadlands hydrothermal area, New Zealand; mineralogy and related geochemistry. Am. J. Sci., v. 269, p. 97-131.

Buchanan, L.J. (1981) Precious-metals deposits associated with volcanic environments in the southwest; in Dickinson, W.R. and Payne, W.D. (eds.), Relations of Tectonics to Ore Deposits in the South Cordillera. Arizona Geological Society Digest, v. 14, p. 237-262.

Choi, S.G., Park, M.E., and Choi, S.H. (1994) Chemical variation of electrum from gold and/or silver deposits in Southeast Korea. Jour. Korean Inst. Mining Geo., v. 27, p. 325-333. (Korean)

Cline, J.S., Bodnar, R.J., Rimstidt, J.D. (1992) Numerical simulation of fluid flow and silica transport and deposition in boiling hydrothermal solutions: application to epithermal gold deposits. J. Geophys. Resc. v. 97, p. 9085-9103.

Cooke, D.R. and McPhail, D.C. (2001) Epithermal Au-Ag-Te mineralization, Acupan, Baguio district, Philippines: numerical simulations of mineral deposition. Economic Geology, v. 96, p. 109-132.

Drummond, S.E. and Ohmoto, H. (1985) Chemical evolution and mineral deposition in boiling hydrothermal systems. Economic Geology, v. 80, p. 126-147.

Fletcher, C.J.N. (1976) Mineralization within the Gyeongsang Cretaceous Basin, Republic of Korea: London: Institute of Geological Sciences, Anglo Korean Mineral Exploration group, p. 33-47.

Fournier, R.O. (1985) The behavior of silica in hydrothermal solutions; in Berger, B.R. and Bethke, P.M. (eds.), Geology and Geochemistry of Epithermal Systems. Reviews in Economic Geology, v. 2.

Heald, P.M., Foley, N.K., and Hayba, D.O. (1987) Comparative anatomy of volcanic-hosted epithermal deposits: Acid-sulfate and adularia-sericite types. Economic Geology, v. 82, p. 1-26.

Hedenquist, J.W. and Henley, R.W. (1985) The importance of $CO_2$ on freezing point measurements of fluid inclusions: evidence from active geothermal systems and implications for epithermal ore deposition. Economic Geology, v. 80, p. 1379-1406

Helgeson, H.C., Kirkham, D.H. and Flowers, G.C. (1981) Theoretical prediction of the thermodynamic behavior of aqueous electrolytes at high pressures and temperatures. IV. Calculation of activity coefficients, osmotic coefficients, and apparent modal and standard and relative partial modal properties to 600°C and 5 kb. Am. Jour. Sci., v. 281, p. 1249-1516.

Hwang. S.K. (1978) Petrology of Late Cretaceous volcanic rocks in Cheonhwangsan area, Kyeongsangnam-do: Unpub. M.S. thesis, Kyungpook Univ., 93p.

James, L.P., Park, M.E. and Atkinson Jr., W.W. (1999) Ag-Au-Te and pyrophyllite-dumortierite in alteration systems, southernmost Korea. SGA-IAGOD Interantion Meeting "Mineral Deposits: Processes to Processing", v. 1, p. 535-537.

Johnson, J.W., Oelkers, E.H., and Helgeson, H.C. (1992) SUPCRT92: A software package for calculation the standard modal thermodynamic properties of minerals, gases, aqueous, species, and reactions from 1 to 5000 bar and 0 to 1000°C. Computers and Geosciences, v. 18, p. 899-947.

Kim, M.Y. and Shin H.J. (1989) Chemical composition of sphalerite relating to mineralization at the Tongyeong mine, Korea. Jour. Korean Inst. Mining Geol., v. 22, p. 103-115. (Korean)

Larson, P.B. and Tayor, H.P. (1987) Solfataric alteration in the San Juan Mountains, Colorado: oxygen isotope variations in a boiling hydrothermal environment. Economic Geology, v. 82, p. 1019-1036.

Lee, K.Y. (1991) Genetic environments of the Tongyeong gold and silver bearing hydrothermal vein deposit, Korea. Ph.D. thesis, Korea Univ., 139p.

Park, H.I. (1983) Ore and fluid Inclusion of the Tongyeong gold-silver deposits, v. 22, p. 103-115.

Park, M.E., Choi, I.S., and Kim, J.S. (1992) Hydrothermal solution-rhyolite reaction and origin of sericite in the Yugwang Mine. Jour. Korean Inst. Mining Geol., v. 25, p. 225-232. (Korea)

Plumlee, G.S., Leach, D.L., Hofstra, A.H., Landis, G.P., Rowan, E.L. and Viets, J.G. (1994) Chemical reaction path modeling of ore deposition in Mississippi Valley-type Pb-Zn deposits of the Ozark Region, U.S. Midcontinent. Economic Geology, v. 89, p. 1361-1383.

Potter, R.W., III. (1977) Pressure corrections for fluid-inclusion homogenization temperatures based on the volumetric properties of the system $NaCl-H_2O$, U.S. Geol. Survey jour. Research, v. 5, p. 603-607.

Reed, M.H. (1982) Calculation of multicomponent equilibria and reaction processes in systems involving minerals, gases, and an aqueous phase. Geochim. Cosmochim. Acta, v. 46, p. 513-528.

Reed, M.H. (1984) Geology, wall-rock alteration, and massive sulfide mineralization in al Portion of the West Shasta District, California. Economic Geology, v. 79, p.

1299-1318.

Reed, M.H. and Spycher, N.F. (1984) Calculation of pH and mineral equilibria in hydrothermal waters with application to geothermometry and studies of boiling and dilution. Geochim. Cosmochim. Acta, v. 48, p. 1479-1492.

Reed, M.H. and Spycher, N.F. (1985) Boiling, cooling, and oxidation in epithermal systems: a numerical modeling approach. In Geology and Geochemistry of Epithermal Systems: in Berger, B.R. and Bethke, P.M. (eds). Reviews in Economic Geology, v. 2, p. 249-272.

Roedder, E. (1960) Primary fluid inclusions in sphalerite crystals from the OH vein, Creede, Colorado [abs.]. Geological Society of America Bulletin, v. 71, p. 19.

Saunders, J.A. and Schoenly, P.A. (1995) Boiling, colloid nucleation and aggregation, and the genesis of bonanza Au-Ag ores of the Sleeper deposit, Nevada. Mineralium Deposita, v. 30, p. 199-210.

Seward, T.M. (1973) Thio complexes of gold and the transport of gold in hydrothermal ore solutions, Geochim. Cosmochim. Acta, v. 37, p. 379-399.

Shelton, K.L., So, C.S., Haeussler, G.T., Chi, S.J. and Lee, K.Y. (1990) Geochemical studies of the Tongyeong gold-silver deposits, Republic of Korea: evidence of meteoric water dominance in a Te-bearing epithermal system. Economic Geology, v. 85, p. 1114-1132.

Shikazono, N. (1985) A comparison of temperatures estimated from the electrum- sphalerite-pyrite-atgentite assemblage and filling temperatures of fluid inclusions forms epithermal Au-Ag vein-type deposits in Japan, Economic Geology, v. 80, p. 1415-1424.

Spycher, N.F. and Reed, M.H. (1989) Evolution of a Broadlands-type epithermal ore fluid along alternative P-T paths: implications for the transport and deposition of base, precious, and volatile metals. Economic Geology, v. 84, p. 328-359.

So, C.S., Yun, S.T. and Park, M.E. (1995) Geochemistry of a fossil hydrothermal system at Barton Penlnsula, King George Island. Antarctic Science, v. 7, p. 63-72.

Tianfu X. and Pruess, K. (2001) On fluid flow and mineral alteration in fractured caprock of magmatic hydrothermal systems. Jour. of Geophysical Research, v. 106, p. 2121-2138.

Watanabe, Y. and Scott, A.M. (1998) Extreme boiling model for variable salinity of the Hokko low-sulfidation epithermal Au prospect, southwestern Hokkaido, Japan. Mineralium Deposita, v. 33, p. 568-578.

Woitsekhowskaya, M.B. and Hemley, J.J. (1995) Modeling metal transport and deposition in Butte-type hydrothermal systems. Economic Geology, v. 90 p. 1329-1337.

Xu, T. and Karsten, P. (2001) On fluid flow and mineral alteration in fractured caprock of magmatic hydrothermal systems, J. Geophys. Resc. v. 106, p. 2121-2138.

2001년 5월 4일 원고접수, 2001년 12월 19일 게재승인.